# Principal Component Analysis of Body Surface Potential Mapping in Atrial Fibrillation Patients Suggests Additional ECG Lead Locations

Stef Zeemering[1], Theo A R Lankveld[2], Pietro Bonizzi[3], Harry Crijns[2], Ulrich Schotten[1]

[1] Department of Physiology, CARIM, Maastricht, The Netherlands
[2] Department of Cardiology, Maastricht University Medical Centre, Maastricht, The Netherlands
[3] Department of Knowledge Engineering, Maastricht University, Maastricht, The Netherlands

## Abstract

*Atrial fibrillation (AF) is typically detected and analyzed in a non-invasive way using the standard 12-lead ECG. However, AF substrate complexity quantification may be suboptimal using conventional ECG locations. We analyzed high-density body surface potential maps of 75 patients in persistent AF to locate regions where AF complexity was predominantly expressed and to search for potential additional lead locations. Principal component analysis was applied to 1 minute of AF for each patient on the original ECG, TQ segments and extracted atrial activity (AA). Spatial complexity $k_{0.95}$ was higher in AA or TQ segments than in ECG (median $k_{0.95}$, AA:* 13 *components, TQ:* 7*, ECG:* 2*, $p < 0.001$). Normalized variance described by the top 3 principal components was lower in AA and TQ segments (median %, AA:* 85%*, TQ:* 87%*, ECG:* 99%*, $p < 0.001$). Maps of normalized component coefficient energy showed expression of major ECG components concentrated in the region covered by $V_1$–$V_6$, while the major TQ and AA components were more dispersed around the precordial leads, suggesting that non-invasive assessment of AF complexity by the standard 12-lead ECG is suboptimal. Placing additional leads around the precordial leads may improve non-invasive characterization of the AF substrate.*

## 1. Introduction

The standard 12-lead ECG is the default tool for the non-invasive analysis of atrial fibrillation (AF), first of all to detect AF, but more and more to quantify the complexity of AF and to guide management of AF [1]. An important question is whether the 12-lead configuration provides the optimal set of leads to capture the relevant aspects of AF complexity, or that other locations on the body surface contain additional information. The body surface potential map (BSPM) is a technique that records an ECG on many sites on the thorax. It has been shown to be a promising tool in guiding AF ablation [2], but its role in the day-to-day AF care remains limited because of the extra effort and costs involved. It does provide a possibility to locate regions of distinct atrial activity on the body surface and perhaps to select an optimal smaller subset of leads to represent the spatial variability of the manifestation of AF on the body surface. Several studies already looked into this question of body surface electrode information content and optimal ECG lead selection [3] [4] [5], but either on a different arrhythmia or based on a relatively low BSPM resolution. Similar to the approach taken in [6], we performed principal component analysis (PCA) on the extracted atrial activity (AA) of high resolution BSPMs (184 leads) of patients in persistent AF to locate regions with strong expression of principal AA components, to quantify the ability of the precordial leads to capture these components, and to find additional leads that improve the expression of the spatial variability of AF.

## 2. Methods

### 2.1. BSPM data and pre-processing

BSPMs were recorded in 75 patients in persistent AF using a custom configuration of 184 leads with 120 anterior and 64 posterior leads (ActiveTwo BSM Panels Carbon Electrodes, Biosemi B.V., The Netherlands), as shown in Figure 1. ECGs were recorded at a 2048Hz sampling frequency. A one-minute segment was selected for each subject, low-quality leads were excluded (low signal-to-noise ratio, poor electrode contact, motion artefacts), and Wilson's Central Terminal was subtracted in line with conventional ECG analysis. After band-pass filtering the signals between 1 and 100Hz (3rd order Chebyshev), QRST cancellation was performed using an adaptive singular value decomposition method, inspired by the approach in [7], with multiple QRST window templates defined using hierarchical clustering. The extracted atrial signals were post-filtered with a 3Hz zero-phase highpass filter (3rd order

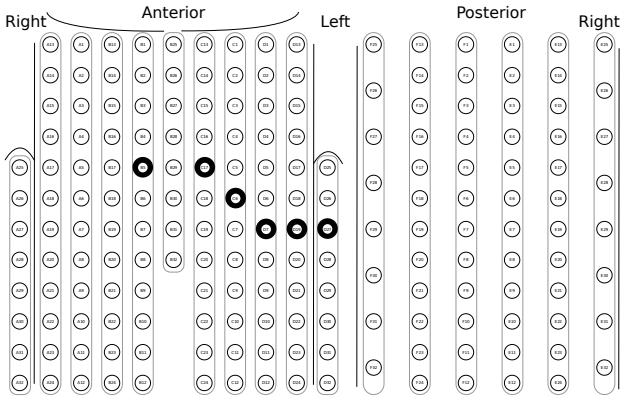


Figure 1: Body surface potential mapping electrode configuration, comprising 120 anterior leads and 64 posterior leads. The default positions of the precordial leads $V_1, \ldots, V_6$ are marked with a thick circle.

Chebyshev) to remove low-frequency residuals not related to (persistent) AF. For the analysis of TQ segments, T-wave fiducial points were detected with an improved version of Woody's method [8]. TQ segments were then detrended using linear interpolation.

## 2.2. PCA-based computation of AF component regions

The components describing the spatial variability of the BSMP signals were determined by applying PCA on 1) the original (band-pass filtered) ECG signal, 2) the de-trended TQ-segments, and 3) the AA signal. PCA computes a linear transformation of a set of signals into a set of uncorrelated principal components (PC), with the first PC describing the maximum amount of variance within the signals. Given the $L \times N$ matrix $\mathbf{X}$ containing $N$ samples for all $L$ electrodes, PCA can be done by means of singular value decomposition:

$$\mathbf{X} = \mathbf{U}\mathbf{\Sigma}\mathbf{V}^{\mathbf{T}}, \tag{1}$$

where $\mathbf{U}$ and $\mathbf{V}$ are orthogonal $L \times L$ and $N \times N$ matrices containing the left- and right singular vectors. The $L \times N$ matrix $\mathbf{\Sigma}$ is a diagonal matrix containing the sorted singular values $\sigma_i$ that are proportional to the amount of variance expressed by the accompanying PCs in the matrix $\mathbf{V}$. The signal matrix $\mathbf{X}$ is mean-centered before PCA. As in [6], we define the normalized variance explained by the *i*th PC to be:

$$\hat{\sigma_i^2} = \frac{\sigma_i^2}{\sum_{i=1}^{L} \sigma_i^2}, \tag{2}$$

and the cumulative variance explained by the first $k$ PCs as:

$$v_k = \frac{\sum_{i=1}^{k} \sigma_i^2}{\sum_{i=1}^{L} \sigma_i^2} = \sum_{i=1}^{k} \hat{\sigma_i^2}. \tag{3}$$

The spatial AF complexity parameter $k_{0.95}$ is computed as the number of components needed to explain at least $95\%$ of the variance in the signals. The mixing matrix $\mathbf{M}$ is the transfer coefficient matrix that quantifies the contribution of each PC in the original signals:

$$\mathbf{M} = \mathbf{U}\mathbf{\Sigma}, \quad \mathbf{X} = \mathbf{M}\mathbf{V}^{\mathbf{T}}. \tag{4}$$

The square of each element of the matrix $M$, $M_{ij}^2$, describes the energy of the *j*th PC in electrode $i$. The relative contribution of the *j*th PC in electrode $i$ can be determined by correcting for the energy of the other PCs:

$$E_{ij} = \frac{M_{ij}^2}{\sum_{j=1}^{L} M_{ij}^2}. \tag{5}$$

By examining this normalized matrix $\mathbf{E}$ we can investigate the distribution of the relative contribution of the dominant PCs on the body surface.

## 2.3. Statistical analysis

Differences in spatial complexity $k_{0.95}$ between the three signal types (ECG, TQ and AA) and cumulative normalized variance $v_k$ were tested with the Friedman test, together with the Dunn-Bonferroni test for pairwise comparisons.

# 3. Results

Spatial complexity $k_{0.95}$ was significantly different between ECG, TQ and AA signals, with high complexity in AA signals, lower complexity in TQ signals, and lowest complexity in ECG signals ($p < 0.001$ for all pairwise comparisons). The cumulative normalized variance of the first three PCs ($v_3$) showed a similar pattern, with almost full variance coverage in the ECG signals and lower coverage in the TQ and AA signals ($p < 0.001$ for all pairwise comparisons). These results are further detailed in Table 1 and Figure 2.

Average maps of component coefficient energy $E_{ij}$ are shown in Figure 3 (last page). They show that in the original ECG signal the first three components are more or less uniformly spread over all electrode locations, with only minor differences between leads. The components are well-represented in the precordial leads. The TQ segments analysis reveals slightly more pronounced regions of dominant component energy, but only in the analysis of the AA component we start to see distinct areas of elevated

Table 1: Spatial complexity and (cumulative) normalized variance for the first three principal components. Values are reported as median (interquartile range).

| Parameter | ECG | TQ | AA | p-value |
|---|---|---|---|---|
| $k_{0.95}$ | 2(0) | 7(3) | 13(7) | $< 0.001$ |
| $v_3$ | 99%(1) | 87%(7) | 85%(8) | $< 0.001$ |
| $\hat{\sigma_1^2}$ | 70%(15) | 48%(14) | 41%(7) | $< 0.001$ |
| $\hat{\sigma_2^2}$ | 26%(15) | 23%(7) | 24%(5) | 0.055 |
| $\hat{\sigma_3^2}$ | 2%(2) | 14%(6) | 16%(5) | $< 0.001$ |

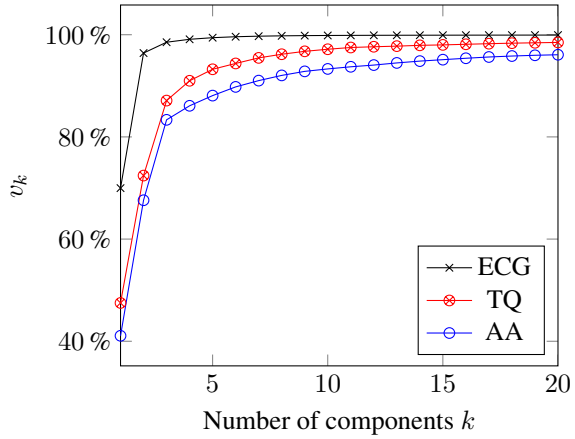


Figure 2: Median cumulative normalized variance $v_k$ as a function of the number of components $k$ for the ECG signal, TQ segments and the extracted atrial activity AA.

component energy. The spread of AA component energy in the interquartile range $[Q_1, Q_3]$ is visualised in Figure 4, which indicates that the normalized variance of the components does vary between patients, but component location is consistent. At first glance, the precordial leads do not necessarily always seem to coincide with these areas of high AA component energy. Table 2 shows the normalized component energy of the precordial leads, which confirms the relatively low presence of especially the first component. Component 2 and 3 are better represented, in lead $V_2$ and leads $V_4 - V_6$ respectively.

Table 2: Normalized AA component energy of the precordial leads and the maximum $V_{max}$ for the first three principal AA components over all precordial leads. Values are given as median $E_{ij}$.

| PC | $V_1$ | $V_2$ | $V_3$ | $V_4$ | $V_5$ | $V_6$ | $V_{max}$ |
|---|---|---|---|---|---|---|---|
| 1 | 23% | 9% | 11% | 10% | 6% | 4% | 40% |
| 2 | 27% | 45% | 33% | 18% | 16% | 15% | 66% |
| 3 | 28% | 15% | 23% | 42% | 45% | 45% | 67% |

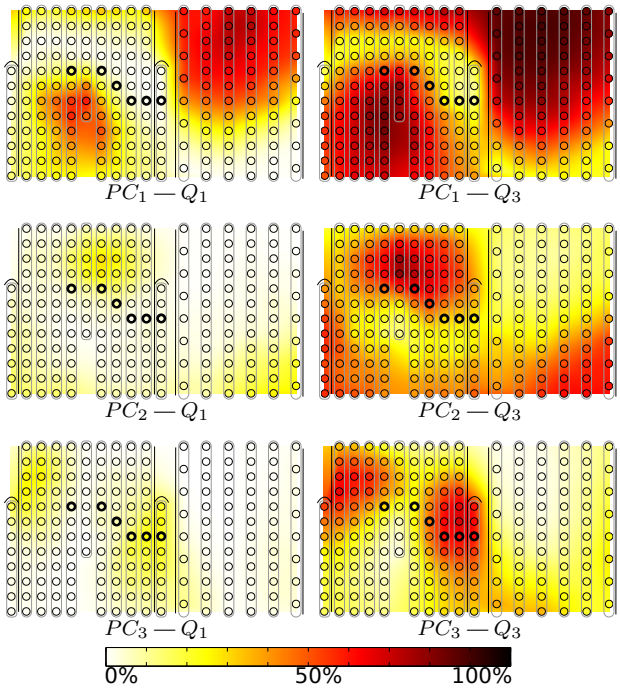


Figure 4: Spread of principal AA component coefficient energy, expressed as the interquartile range $[Q_1, Q_3]$of $E_{ij}$ (in %) for each body surface electrode location.

## 4. Conclusions

Principal component analysis of BSPMs in patients in persistent AF reveals more spatial variability in the atrial signal compared to the original ECG signal. Spatial complexity was significantly higher in AA than in ECG. Averaged maps of normalized component energy reveal at least three distinct components describing spatial variability, both in AA signals as well as - to a lesser extent - in concatenated TQ segments. Overall component energy in the precordial leads is not optimal. First component hot spots are below $V_1$ and on the higher back, above $V_7 - V_9$. The second component is predominantly expressed in $V_2$ and the region above $V_2$. The third component is mainly covered by leads $V_4 - V_6$. Placing additional leads that improve component expression and therefore enhance the description of the spatial variability of AF may lead to better quantification of AF substrate complexity. Further analysis of BSPM data and integration of patient treatment results into the analysis is needed to confirm the relevance of adding the suggested lead locations to the standard 12-lead ECG.

## Acknowledgements

This study was supported by a grant from the European Union (FP7 Collaborative project EUTRAF, 261057).

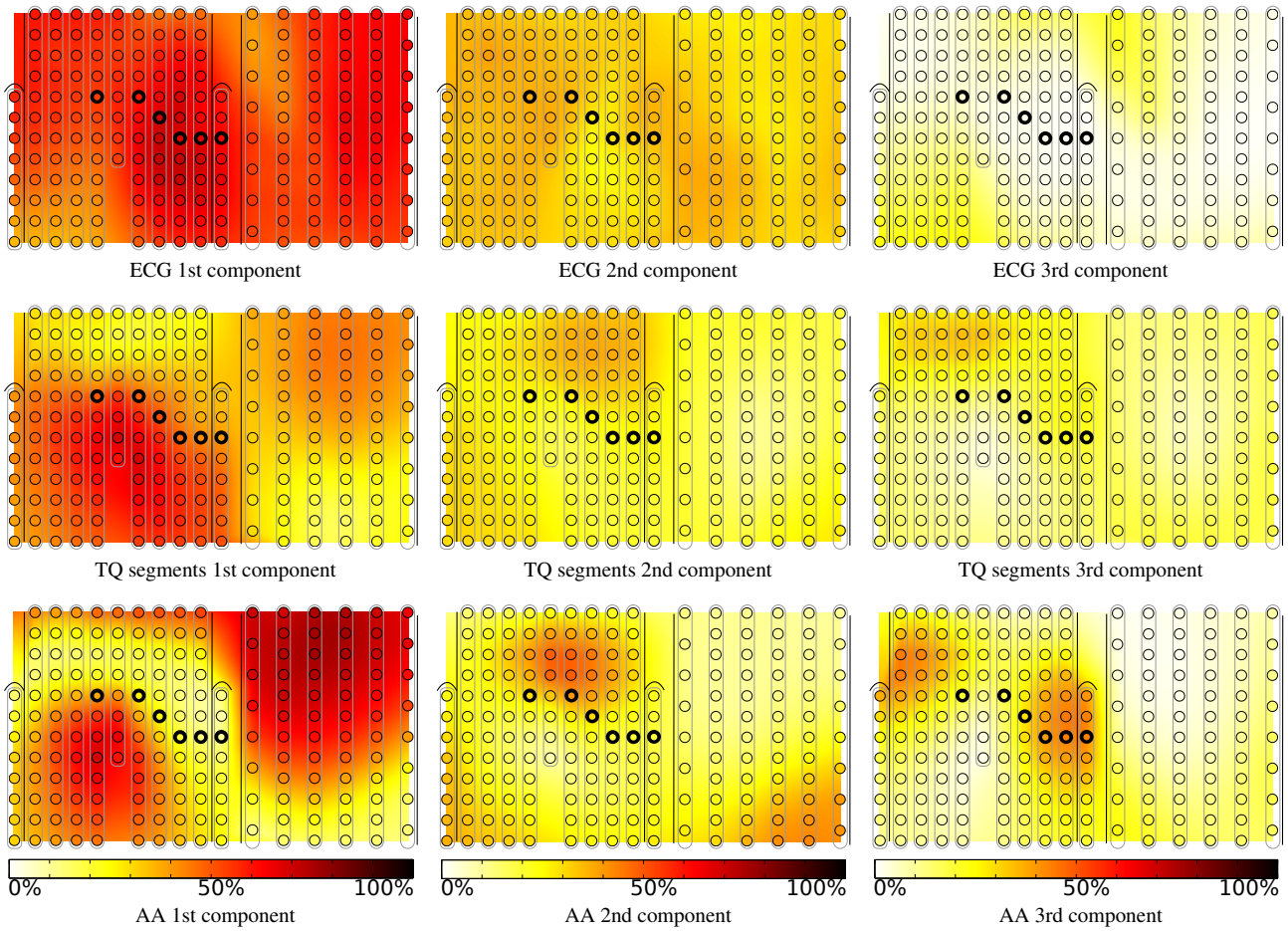


Figure 3: Average component coefficient energy maps, showing average $E_{ij}$ (in %) for each body surface electrode location. Precordial lead locations are marked with a thick circle.

## References


[1] Lankveld TAR, Zeemering S, Crijns HJGM, Schotten U. The ECG as a tool to determine atrial fibrillation complexity. Heart. 2014 Jul;100(14):1077–84.

[2] Hassaguerre M, Hocini M, Denis A, Shah AJ, Komatsu Y, Yamashita S, et al. Driver Domains in Persistent Atrial Fibrillation. Circulation. 2014 Jul; Ahead of print.

[3] Lux RL. Electrocardiographic potential correlations: rationale and basis for lead selection and ECG estimation. Journal of Electrocardiology. 2002;35 Suppl:1–5.

[4] Guillem MS, Castells F, Climent AM, Bod V, Chorro FJ, Millet J. Evaluation of lead selection methods for optimal reconstruction of body surface potentials. Journal of Electrocardiology. 2008 Jan;41(1):2634.

[5] Vanheusden FJ, Li X, Chu GS, Almeida TP, Ng GA, Schlindwein FS. Analysis of spatial variability for the development of reduced lead body surface maps. Computing in Cardiology; 2013:535–8.

[6] Bonizzi P, Guillem M de LS, Climent AM, Millet J, Zarzoso V, Castells F, et al. Noninvasive assessment of the complexity and stationarity of the atrial wavefront patterns during atrial fibrillation. IEEE Trans Biomed Eng. 2010 Sep;57(9):2147–57.

[7] Alcaraz R, Rieta JJ. Adaptive singular value cancelation of ventricular activity in single-lead atrial fibrillation electrocardiograms. Physiol Meas. 2008 Oct 22;29(12):1351–69.

[8] Cabasson A, Meste O, Time delay estimation: A new insight into the Woodys method, IEEE Signal Process. Lett. 2008;15:573–576.



Address for correspondence:

Stef Zeemering, Maastricht University, Dept. of Physiology
P.O. Box 616, 6200 MD Maastricht, The Netherlands
s.zeemering@maastrichtuniversity.nl